Biosensors and Bioelectronics 132 (2019) 279–285

Contents lists available at ScienceDirect

Biosensors and Bioelectronics

journal homepage: www.elsevier.com/locate/bios

Tyrosinase-immobilized CNT based biosensor for highly-sensitive detection of phenolic compounds

Youngho Wee[a,1], Seunghwan Park[a,1], Young Hyeon Kwon[a,1], Youngjun Ju[a], Kyung-Min Yeon[b], Jungbae Kim[a,*]

[a] Department of Chemical and Biological Engineering, Korea University, Seoul 02841, Republic of Korea
[b] Engineering Center, Samsung C&T Corporation, Tower B, 26, Sangil-ro 6-gil, Gangdong-gu, Seoul 05288, Republic of Korea

ARTICLE INFO

Keywords:
Enzymatic biosensor
Tyrosinase
Carbon nanotubes
Enzyme adsorption, precipitation and crosslinking
Phenolic compounds, Screen-printed electrode

ABSTRACT

Highly sensitive phenol biosensor was developed by using well-dispersed carbon nanotubes (CNTs) in enzyme solution and adding CNTs in enzyme electrodes. First, the intact CNTs were dispersed in aqueous tyrosinase (TYR) solution, and TYR molecules were precipitated and crosslinked to prepare the sample of enzyme adsorption, precipitation and crosslinking (EAPC). EAPC exhibited 10.5- and 5.4-fold higher TYR activity per mg of CNTs as compared to enzyme adsorption (EA) and enzyme adsorption/crosslinking (EAC), respectively. EAPC retained 29% of its initial activity after incubation at 40 °C for 128 h, while EA and EAC showed no residual activities, respectively. In biosensing a model phenolic compound of catechol, the sensitivities of EA, EAC and EAPC electrodes on glassy carbon electrode (GCE) were 34, 281 and 675 μA/mM/cm^2, respectively. When 90 w/w% CNTs were added to the enzyme electrodes, the sensitivities of EA, EAC, and EAPC electrodes were 146, 427, and 1160 μA/mM/cm^2, respectively, and the EAPC electrode showed a 2.3-fold increase in sensitivity upon CNT addition. Catechol and phenol could also be detected by EAPC on the screen-printed electrode (SPE), with sensitivities of 1340 and 1170 μA/mM/cm^2, respectively. The sensitivity of EAPC-SPE for phenol detection in the effluent from real municipal wastewater treatment plant was 1100 μA/mM/cm^2. The sensitivity of EAPC-SPE retained 74% of its initial sensitivity after incubation at 40 °C for 12 h. The combination of EAPC immobilization and CNT addition has great potential for application in the development of sensitive enzyme biosensors for various analytes and phenols in water environments.

1. Introduction

Environmental monitoring of pollutants, which have adverse effects on ecosystems and human health, has contributed to the sustainable management of water resources for society. Traditional analytical methods like high-performance liquid chromatography (HPLC) (Alarcón et al., 1987; Angelino and Gennaro, 1997; Cheaib et al., 2018; Williamson et al., 2002) coupled with mass spectrometry (Sczesny et al., 2003) or capillary electrophoresis (Martínez et al., 2000) have been employed as reference methods. However, these traditional methods present drawbacks in terms of expensive reagents, sample pretreatment, and expensive equipment (Cheaib et al., 2018). Thus, the development of sensor devices with high sensitivity and stability are urgently needed. In that sense, the enzymatic biosensors have been widely employed because of its potential to detect a target substance/analyte with high specificity via enzyme-catalyzed reactions (Badihi-Mossberg et al., 2007; Baeumner, 2003; Shahar et al., 2019; Wu et al., 2012)

The detection of phenolic compounds is of great importance due to their presence in a broad range of chemical manufacturing processes and their toxicities (Švitel, 1998; Tang et al., 2008). Tyrosinase (TYR) has been examined for use in electrochemical biosensors that can specifically detect phenolic compounds (Camargo et al., 2018; Cerrato-Alvarez et al., 2019; Tsai and Chiu, 2007; Vicentini et al., 2013). Briefly, TYR catalyzed the oxidation of phenolic compounds to quinone species, which can be further reduced at the enzyme electrode to generate electrochemical signals (Dai et al., 2016; Yamazaki and Itoh, 2003). This TYR-catalyzed oxidation allows electrochemical detection of phenolic compounds at low potentials, where redox reactions of the interfering species are insignificant (Kurbanoglu et al., 2017; Zhou et al., 2014).

One of the crucial factors in the potential success of enzyme-based

* Corresponding author.
E-mail address: jbkim3@korea.ac.kr (J. Kim).
[1] These authors contributed equally to this work.

https://doi.org/10.1016/j.bios.2019.03.008
Received 5 December 2018; Received in revised form 5 March 2019; Accepted 6 March 2019
Available online 07 March 2019
0956-5663/

phenol biosensors is the immobilization and stabilization of TYR. Nanobiocatalysis, using various nanomaterials for enzyme immobilization, has been proven as a highly effective approach, enhancing the loading and stability of enzymes compared to conventional enzyme immobilization (Datta et al., 2013; H. Kim et al. 2017; J.H. Kim et al. 2011; Kim et al. 2006, 2008; J.-H. Kim et al. 2017; Lee et al., 2014, 2017). In particular, nanobiocatalytic strategies using conductive nanomaterials such as carbon nanotubes (CNTs) and polyaniline nanofibers have demonstrated high sensitivity and long-term stability of enzyme electrodes in various applications of electrochemical biosensors (H. Kim et al. 2011; Kim et al. 2008, 2015; Kwon et al., 2010; Lai et al., 2016). CNTs are one of the best candidates for enzyme immobilization because they provide large surface areas for effective enzyme loading and exhibit biocompatibility (Shim et al., 2002; Zhang and Henthorn, 2009). In the electrochemical application of enzymes, CNTs offer unique advantages with their extraordinary electronic properties (Barone et al., 2004; Tîlmaciu and Morris, 2015; Willner et al., 2009), such as faster electron transfer kinetics than traditional carbon electrodes (Jacobs et al., 2010). Recently, we reported a unique method of enzyme immobilization on intact CNTs without acid treatment, based on the good dispersion of CNTs in the glucose oxidase solution for biofuel cell application (B.C. Kim et al., 2017).

In this present work, we developed TYR-based biosensors for highly sensitive detection of phenolic compounds (Fig. 1). Intact CNTs were first dispersed in aqueous TYR solution, and TYR was immobilized onto intact CNTs via the enzyme adsorption, precipitation, and crosslinking (EAPC) approach. Two control immobilization formulations of enzyme adsorption (EA) and enzyme adsorption and crosslinking (EAC) were prepared for comparative studies in enzyme activity and stability, together with the characteristics of enzyme electrodes. Particularly, the sensitivity of enzyme electrodes was checked by using a model phenolic compound of catechol. To improve the sensitivity further, intact CNTs were added to the enzyme electrodes, which can facilitate electron transfer between immobilized TYR molecules to the main electrode of the glassy carbon electrode (GCE) or screen-printed electrode (SPE). In particular, the SPE was employed to demonstrate the potential of the EAPC electrode to be used for in-situ environmental monitoring of phenolic compounds.

2. Material and methods

2.1. Materials

Tyrosinase from mushroom (EC 1. 14. 18. 1), pyrocatechol, phenol, sodium phosphate monobasic, sodium phosphate dibasic, Tris-HCl, Trizma base, glutaraldehyde (GA, 25%), ammonium sulfate, reduced graphene oxide (rGRO), and Nafion® (5 wt%) were purchased from Sigma Aldrich (St Louis, MO, USA). All solutions were prepared using deionized water (DI, 18.2-MΩ cm resistivity) from a Milli-Q water purification system (Millipore Corp., Bedford, MA, USA). Carbon nanotubes (CNTs, multi-walled, 30 ± 15 nm in outer diameter and 1–5 μm in length, purity > 95%) were purchased from Nanolab, Inc. (Newton, MA, USA).

2.2. Tyrosinase immobilization on carbon nanotube via EA, EC and EAPC methods

Intact CNTs were used for the immobilization of TYR, and three different approaches were employed to immobilize TYR onto CNTs: EA, EAC, and EAPC. For the preparation of EA, 4 mg CNTs in 1 mL of sodium phosphate buffer (PB, 100 mM, pH 6.5) were mixed with 1 mL of 10 mg/mL TYR solution in 100 mM PB (pH 6.5). The mixture was sonicated a few times for 10–30 s and incubated at room temperature under shaking (200 rpm) for 1 h, and under rocking (50 rpm) at 4 °C overnight. EAC was prepared by adding 25% GA to the mixture of CNTs and TYR solution to make the final concentration of 0.5% (w/v) GA. This sample was also incubated under rocking (50 rpm) condition at 4 °C overnight. To prepare EAPC, ammonium sulfate (40%, w/v) was added to the mixture of CNTs and TYR solution to induce the precipitation of TYR. After shaking (200 rpm) at room temperature for 30 min, the GA solution was added to the mixture to make a concentration of 0.5% (w/v), and the mixture was incubated at 4 °C under

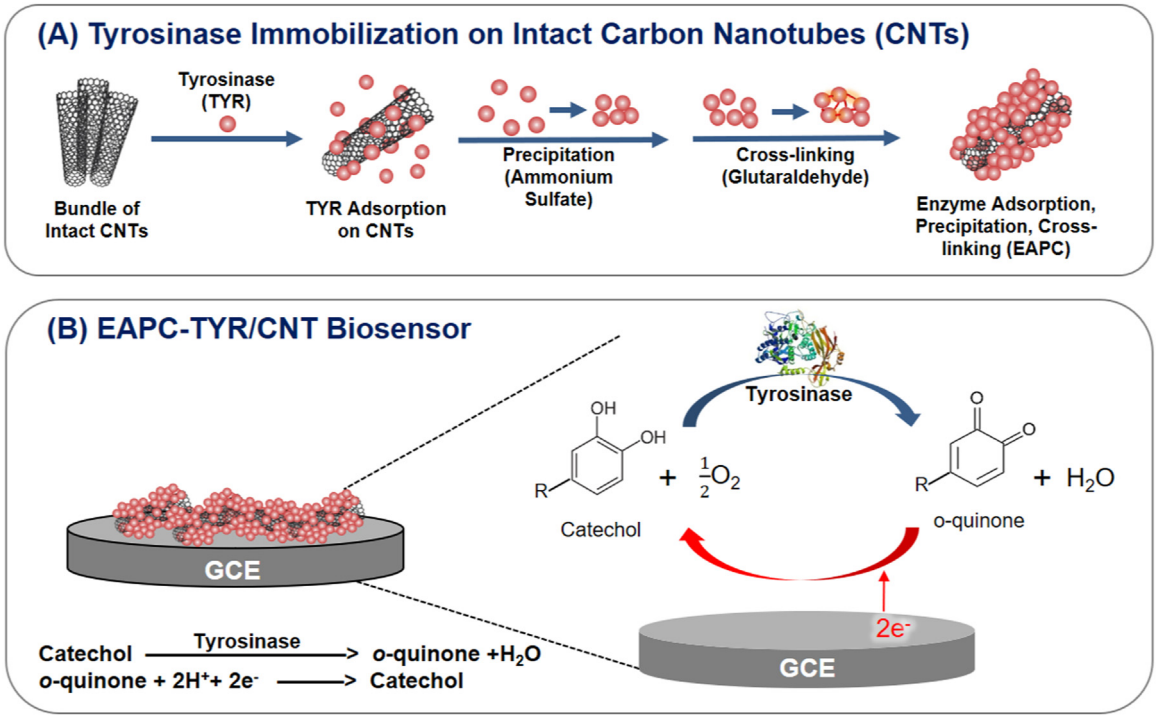

Fig. 1. Schematic illustrations of (A) EAPC protocol, consisting of enzyme adsorption, precipitation, and crosslinking, and (B) electrochemical reactions occurring in the EAPC electrode on glassy carbon electrode.

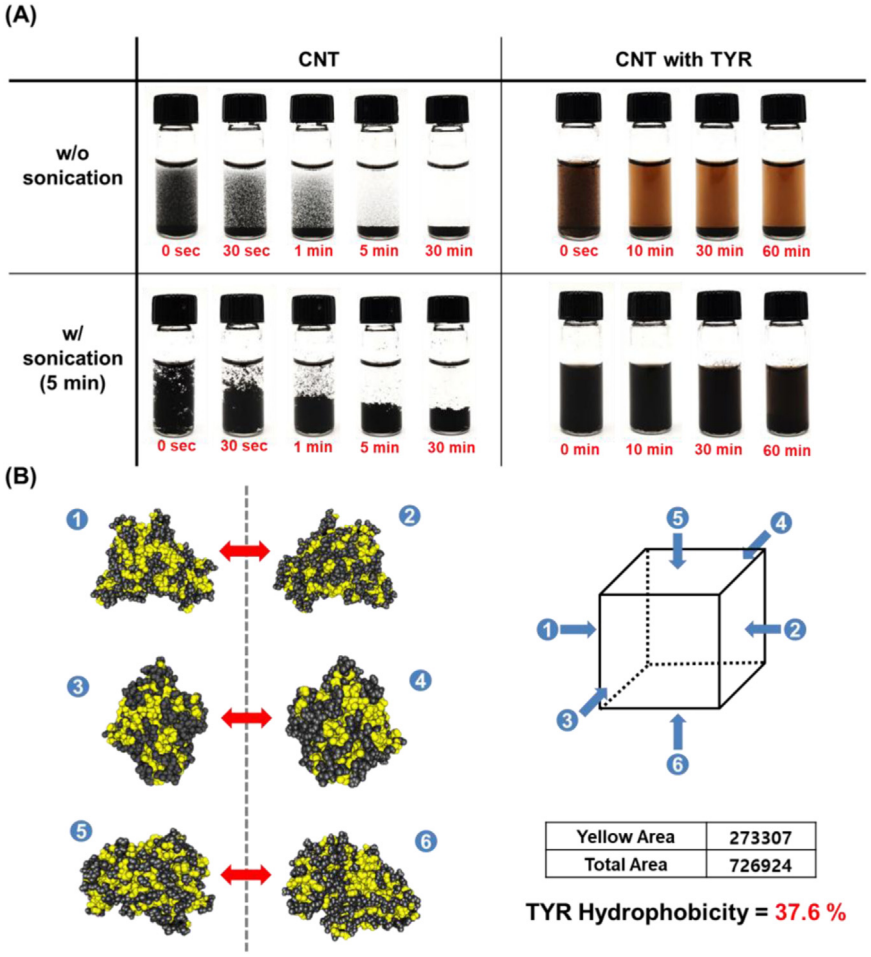

Fig. 2. (A) Dispersion of intact CNTs in aqueous TYR solution. Both TYR in solution and sonication are needed for the good dispersion of CNTs in aqueous solution. (B) Surface hydrophobicity of TYR molecules. Hydrophobic side chains of valine, leucine, isoleucine, phenylalanine and glycine are marked in yellow spheres, while the others are marked in gray spheres. The surface of TYR molecule was viewed from six orthogonal angles, and the surface hydrophobicity was calculated by ratio of hydrophobic area to total enzyme surface area. Each area was measured by pixels using Adobe Photoshop (San Jose, CA, USA).

rocking (50 rpm) overnight. To cap the unreacted aldehyde groups, the samples were treated with 100 mM Tris-HCl buffer (pH 7.4) under shaking (200 rpm) for 30 min and were washed three times using 10 mM PB (pH 6.5). EA, EAC, and EAPC were stored in 100 mM PB (pH 6.5) at 4 °C until use. To compare EA, EAC, and EAPC, the amount of immobilized TYR samples is represented by the weight of CNTs to be used for their immobilization.

2.3. Activity and stability measurements of TYR-immobilized CNTs

The activity of the immobilized TYR samples was measured following the protocol of Naidja et al. (Naidja et al., 1999), using the TYR-catalyzed oxidation of catechol. To initiate the reaction of TYR catalysis, 500 µL of TYR-immobilized CNT sample solution was added to 4.5 mL of 5 mM catechol solution, and the mixtures were shaken (200 rpm) at 25 °C. The sodium phosphate buffer (PB, 100 mM, pH 6.5) was used to make the solution of both TYR and catechol. To measure the activity, 200 µL of reaction cocktail was taken at each time point and mixed immediately with 800 µL of 100 mM PB (pH 6.5) in a cuvette. The absorbance (394 nm) at each time point was measured using a spectrophotometer (UV-1800, Shimadzu, Kyoto, Japan). The activity of immobilized-TYR sample was determined by the initial slope of the time-dependent absorbance increase.

To check the stability, TYR samples prepared by EA, EAC, and EAPC approaches were stored in 100 mM PB (pH 6.5) at 40 °C. At each time point, the TYR activity was measured by the catechol oxidation, and the relative activity was calculated by the ratio of residual activity at each time point to the initial activity of each sample.

2.4. Preparation of enzyme electrodes using EA, EAC, and EAPC

Enzyme electrodes were fabricated on glassy carbon electrode (GCE, 3 mm diameter, CH Instruments Inc., Austin, TX, USA) and screen-printed electrode (SPE, DropSens, Oviedo, Spain). GCE was polished with alumina and washed with DI water. EA, EAC, and EAPC at a final CNT concentration of 1 mg/mL were dispersed in Nafion® solution (0.5 wt%). For the enhancement of the electron transfer rate, CNTs and rGRO were dispersed in 100 mM PB (pH 6.5) buffer, sonicated a few times for 10–30 s, and added to the solution containing TYR samples and Nafion® at 90% w/w of CNTs or rGRO. The suspension (20 µL) was dropped onto the GCE and SPE surface and allowed to dry under ambient conditions for 0.5–1 h. Electrodes were immersed in 10 mL of 100 mM PB (pH 6.5) for catechol detection.

2.5. Electrochemical performance measurements

An electrochemical workstation (CHI 760C) from CH Instruments (Austin, TX, USA) was used to measure the amperometric response of TYR-immobilized CNT electrode to the addition of catechol. Ag/AgCl electrode and a platinum wire electrode were used as reference electrode and counter electrode, respectively. The diameter and length of the platinum counter electrode were 0.5 and 32 mm, respectively. An

external potential of −0.1 V vs. Ag/AgCl was applied as the operating potential for the amperometric test of TYR electrodes. After a 1 h stabilization of the current response, the steady current responses of EA, EAC, and EAPC were measured under magnetic stirring (400 rpm). The catechol solution (10 μL of 0.5 mM catechol) was added into the 10 mL of 100 mM PB (pH 6.5) in a successive manner in intervals of 5 min, and its current signal was subsequently obtained. The calibration plots were constructed from this current signal-catechol concentration data, and their linear ranges were used to estimate the sensitivity of the EA, EAC, and EAPC electrodes. Cyclic voltammetry (CV) measurements were carried out on glassy carbon electrodes (GCE) by using a CHI 760C electrochemical workstation. The measurements were based on a three-electrode system, consisting of the modified GC electrode as the working electrode, an Ag/AgCl electrode as the reference electrode, and a platinum wire as the auxiliary electrode.

3. Results and discussion

3.1. Dispersion of CNTs with TYR

CNTs with no acid treatment did not exhibit good dispersion in water as they settled down very quickly, while the sonication of CNTs did help to improve the thickness of the CNT layer, despite their settling. This can be explained by the improvement in the reaction of metal catalysts in the CNT sample with water molecules upon sonication. On the other hand, the addition of CNTs into the TYR solution and the following simple sonication resulted in the good dispersion of CNTs in the aqueous buffer solution (100 mM PB, pH 6.5) (Fig. 2A). We report a similar observation of CNT dispersion in the aqueous solution of glucose oxidase (GOx), which was explained by the hydrophobic interaction between CNTs and hydrophobic amino acid residues on the surface of GOx molecules (B.C. Kim et al., 2017). As an extension, we checked the surface hydrophobicity of the TYR molecule by depicting the side chains of hydrophobic amino acids (alanine, valine, leucine, isoleucine, methionine, phenylalanine, tryptophan, proline, and glycine) with yellow spheres and the other parts with gray-colored spheres (Fig. 2B) in the enzyme structure obtained from protein data bank (TYR, PDB ID: 5M6B). We estimated the coverage of surface hydrophobicity on the TYR molecule by checking the six different images taken from six orthogonal angles, which were orthogonal to one another. Surface analysis based on counting pixels reveals that the hydrophobic coverage on the surface of TYR and GOx molecules were 36.7% and 28.2%, respectively (Fig. S1). This analysis supports the good dispersion of CNTs in the TYR solution, as well as in the GOx solution, based on the amphiphilic properties of the TYR molecule. In other words, the hydrophobic patch on the surface of the TYR molecule would be able to interact with the highly hydrophobic surface of intact CNTs, while the hydrophilic side chains on the surface of TYR, represented by gray spheres, can interact with hydrophilic water molecules, facilitating the dispersion of CNTs in an aqueous TYR solution.

3.2. Activity and stability of immobilized TYR on CNTs

CNTs, well dispersed in the TYR solution, were used for the immobilization of TYR via the three different approaches of EA, EAC, and EAPC. Fig. 1A schematically shows the preparation of EAPC on CNTs, which consists of TYR adsorption on CNTs, precipitation, and crosslinking. The first step of TYR adsorption on CNTs represents the well-dispersed CNTs in the TYR solution (Fig. 2A). EAC is the control of EAPC, prepared via enzyme adsorption and crosslinking, without the step of enzyme precipitation. The TYR activity was measured by checking the oxidation rate of catechol. As shown in Fig. 3A, the activities of EA, EAC, and EAPC were 2.4, 4.6, and 25 ΔA_{394}/min per 1 mg of CNTs, respectively. The activity of EAPC was 10.5- and 5.4-fold higher than those of EA and EAC, respectively. The higher activity of EAPC can be explained by the higher enzyme loading per unit weight of

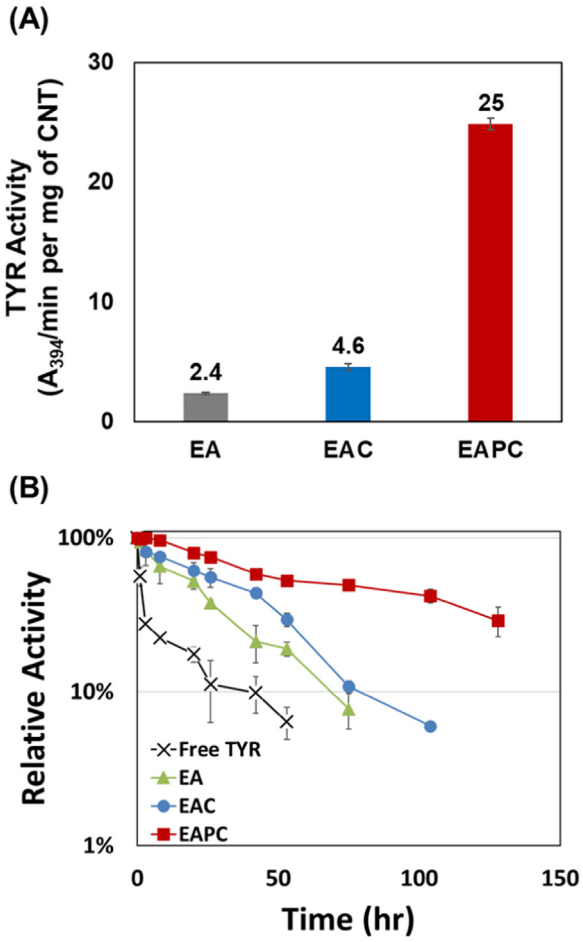

Fig. 3. (A) The activity of EA, EAC, and EAPC. (B) The thermal stability of free TYR, EA, EAC, and EAPC. The samples were incubated in an aqueous buffer solution at 40 °C.

CNTs due to the effective enzyme crosslinking after enzyme precipitation. In other words, the addition of ammonium sulfate precipitates the enzyme molecules, and the precipitated enzyme molecules in close contact with one another would be cross-linked in a more effective way, leading to the higher enzyme loadings of EAPC.

The enzyme loadings of EAC and EAPC are difficult to estimate because conventional protein assays are based on soluble form of enzymes and the insoluble form of crosslinked enzymes cannot be measured. As a bypass, elemental analysis was performed to measure the amount of nitrogen atom, which can be used to calculate the enzyme loading of each sample. According to elemental analysis, the enzyme loadings of EA, EAC, and EAPC were estimated to be 0.43, 0.93, and 12.8 mg of tyrosinase on 1 mg of CNTs, respectively. In other words, the enzyme loading of EAPC was 30 and 14 times higher than those of EA and EAC, respectively. The specific enzyme activities of EA, EAC and EAPC were calculated to be 5.6, 4.9, and 1.9 ΔA_{394}/min per 1 mg of immobilized tyrosinase. The lower specific activity of EAPC than those of EA and EAC can be explained by the structural enzyme deformation upon enzyme crosslinking as well as more serious mass transfer limitation due to a lot higher enzyme loading of EAPC than EA and EAC.

The stability of EA, EAC, and EAPC was checked by measuring the time-independency of the TYR activity after sample incubation at 40 °C. The relative activity represents the ratio of residual activity at each time point to the initial activity of each sample. Free TYR, EA, and EAC all showed a rapid decrease in TYR activity, while EAPC exhibited fairly good stabilization of enzyme activity by maintaining a relative activity of 29% after 128 h. The improved stability of EAPC can be explained by

the effective enzyme crosslinking that forms a greater number of chemical linkages on the surface of TYR molecule and inhibits the TYR denaturation and leaching from CNTs in a more efficient way. Interestingly, the inactivation curves of immobilized TYR samples show biphasic inactivation curves with two different linear correlations in the semi-log-scale plot (Fig. 3B). In other words, the rapid inactivation was followed by the slower inactivation kinetics. This biphasic pattern of enzyme inactivation is fairly common when chemical treatment, such as enzyme cross-linking, is performed (B.C. Kim et al. 2011; Kim et al. 2018; Lee et al., 2017). The labile population, with fewer numbers of chemical linkages, are inactivated in the first phase of enzyme inactivation, while the highly stabilized population, with greater numbers of chemical linkages, are inactivated at a later phase.

3.3. Electrochemical performance of EA, EAC, and EAPC biosensors without and with additional CNTs

To demonstrate the potential application of TYR-immobilized CNTs, the enzyme electrodes were prepared by entrapping EA, EAC, and EAPC onto glassy carbon electrodes utilizing Nafion® binder. The sensitivities of EA, EAC, and EAPC electrodes were determined from the slope of the current response by adding the catechol solution in a successive manner. To check the catechol reduction, the potential was fixed at −0.1 V vs. Ag/AgCl over the enzyme electrode. The following equations show the catechol oxidation catalyzed by TYR (Eq. (1)) together with the follow-up *o*-quinone reduction to catechol (Eq. (2)).

$$\mathbf{Catechol} \xrightarrow{\text{tyrosinase}} \boldsymbol{o} - \mathbf{quinone} + \mathbf{H_2O} \quad (1)$$

$$\boldsymbol{o} - \mathbf{quinone} + \mathbf{2H^+} + \mathbf{2e^-} \rightarrow \mathbf{Catechol} \quad (2)$$

The sensitivities of EA, EAC, and EAPC electrodes were 146, 427, and 1160 μA/mM/cm^2, respectively (Fig. 4, Fig. S2A, and Table S2). The EAPC electrode exhibited 7.9- and 2.7-fold higher sensitivity than the EA and EAC electrodes, respectively, which can be partially explained by the higher enzyme activity of EAPC compared to EA and EAC (Fig. 3A and Table S1).

To improve the electron transfer rate in the enzyme electrodes, we add free CNTs or rGRO with no enzyme immobilization to the EA, EAC, and EAPC electrodes, and the electrochemical performance of each enzyme electrode was checked. With a fixed amount of enzyme immobilized CNTs (2 μg), the sensitivities of EA, EAC, and EAPC with the addition of free CNTs (18 μg, 90 w/w% CNTs addition) were 139, 159, and 2710 μA/mM/cm^2, respectively (Fig. 4, Fig. S2B and Table S1). Interestingly, the addition of free CNTs improved the sensitivity of the EAPC electrode only, while the other EA and EAC electrodes showed little change or even lowered sensitivity upon the addition of free CNTs. The improved sensitivity of the EAPC electrode upon CNT addition can

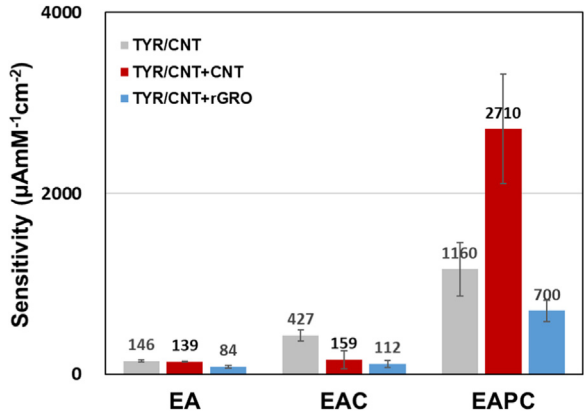

Fig. 4. The electrochemical sensitivity of TYR electrodes with and without additional CNTs and rGRO (90 w/w%).

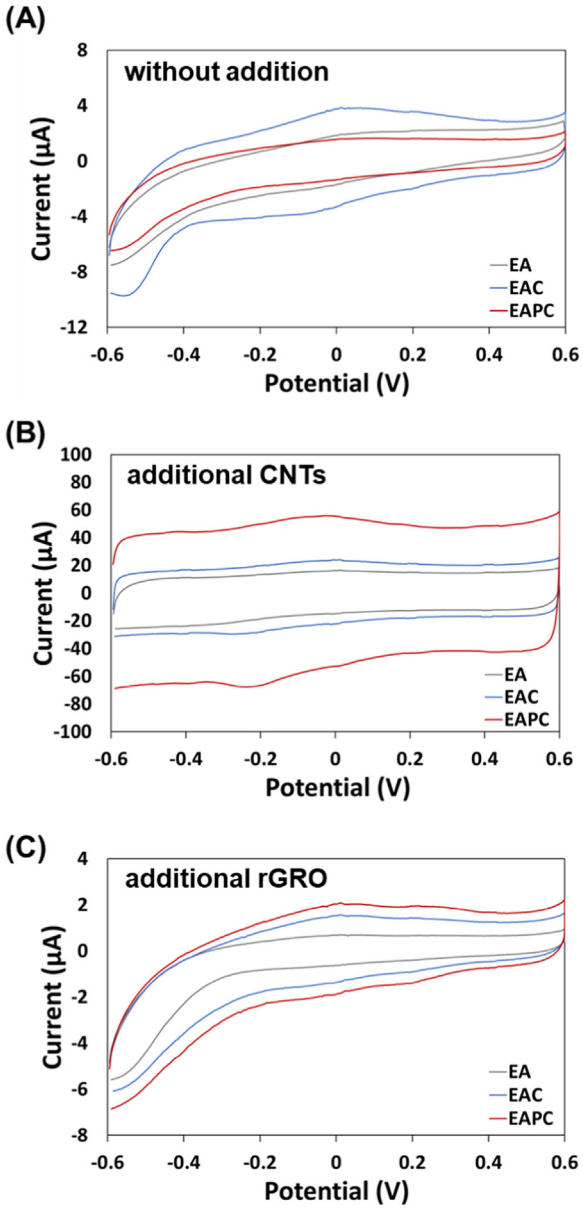

Fig. 5. CVs of EA, EAC, and EAPC electrodes without CNTs (A), with additional CNTs (B), and with additional rGRO (C). The scan rate was 50 mV/s.

be explained by the improved electron transfer from the main electrode of GCE to *o*-quinone, generated from TYR-catalyzed catechol oxidation. In other words, EAPC generates much more *o*-quinone because of its higher TYR activity than EA and EAC, but the EAPC electrode without additional CNTs cannot effectively transfer electrons from GCE to *o*-quinone. This leads to the accumulation of *o*-quinone, which can be effectively reduced to catechol because of the improved electron transfer rate via the electron highway induced from the additional 90 w/w% CNTs. Interestingly, upon addition of rGRO (18 μg, 90 w/w%), the sensitivities of EA, EAC, and EAPC electrodes were reduced to 84, 112, and 700 μA/mM/cm^2, respectively (Fig. 4, Fig. S2C, and Table S2), which can be explained by the interference of mass transfer by the 2D structure of rGRO.

Fig. 5 shows the cyclic voltammograms (CVs) of EA, EAC, and EAPC electrodes with and without additional CNTs or rGRO. With neither CNTs nor rGRO added, the peak current of EAC is greater than those of EA and EAPC. The lower peak current of EAPC compared to EAC can be explained by the increased loading of non-conductive enzymes on CNTs

in the immobilization of EAPC. The activity of EAPC were 10.5- and 5.4-fold higher than that of EA and EAC, respectively, while the sensitivity of EAPC were 7.9- and 2.7-fold higher than that of EA and EAC, respectively. The activity ratios of EAPC electrode to the EA and EAC electrodes were lower than the activity ratios of EAPC to EA and EAC immobilization. The sensitivity of the TYR electrode is determined by a series of enzymatic catechol oxidation and electron transfer reactions from the main electrode (GCE) to *o*-quinone in its reduction to catechol. Then, the lower sensitivity ratios compared to the activity ratios of EAPC to EA and EAC can be potentially explained by the reduced electron transfer of EAPC electrode, which consists of thicker enzyme cluster compared to EA and EAC electrodes. According to the CV results, the peak current of EAC is higher than both EA and EAPC (Fig. 5A). The lower peak current of EA compared to EAC reveals the reduced amount of adsorbed enzyme molecules upon rigorous washing for EA, which potentially induces the re-aggregation of CNTs through the lack of a sufficient number of enzyme molecules to prevent it. Having said that, the higher peak current of EAC than both EA and EAPC suggests that EAC has sufficient enzyme molecules to prevent the serious aggregation of CNTs with EA and the immobilization of high enzyme loading with EAPC.

When intact CNTs were added to the enzyme electrodes, the peak currents of EA, EAC, and EAPC electrodes were all increased, which reflects the improved electron transfer rate upon the addition of CNTs. With 90 w/w% CNTs added, the sensitivities of EA, EAC, and EAPC 139, 159, and 2710 μA/mM/cm^2, respectively, which were higher than those with no CNTs added by factors of 0.95, 0.37, and 2.3, respectively (Table S2). In other words, the largest amount of TYR loading resulted in the highest rate of *o*-quinone formation, in which *o*-quinone would accumulate in an inefficient electron conductive system with no addition of CNTs. The addition of intact CNTs can play a role in the effectiveness of the electron transfer highway, which can improve the rate of electron transfer between GCE and *o*-quinone. Against expectations, the peak currents of all EA, EAC, and EAPC electrodes decreased upon the addition of 90 w/w% rGRO. This result reveals the adverse role of rGRO as a blockade against the mass transfer of catechol and *o*-quinone.

To develop sensitive TYR electrodes for field or point-of-contact tests (Fig. S3), we used SPE to fabricate the enzyme electrode of EAPC with 90% CNTs (Fig. 6). The sensitivities of EAPC electrodes with additional CNTs on SPE were 1340 and 1170 μA/mM/cm^2 in the detection of catechol and phenol, respectively. The linear ranges of EAPC with additional CNTs for catechol and phenol were 1.5–8 and 0.5–5.5 μM, respectively. The limits of detection (LODs) were calculated based on the standard deviation of response and slope method, and the LODs of EAPC with additional CNTs were 14 and 35 nM for catechol and phenol, respectively (Fig. 6A). At an applied potential of −0.1 V vs. Ag/AgCl, the detection sensitivity of phenol is lower than that of catechol (Dalkıran et al., 2017; Portaccio et al., 2006; Tsai and Chiu, 2007) because one more step of phenol oxidation to catechol is required. The high sensitivity of EAPC on SPE for phenol compounds has demonstrated its potential to be employed for easy and simple field tests to detect toxic compounds in water environments. Furthermore, we investigated the specificity of EAPC with additional CNTs on SPE by injection of 5 different chemicals (catechol, phenol, glucose, sucrose, and diphenylamine), which have similarity in structure or size and potentially exist in waste water. Only the target compounds of catechol and phenol could give us a decent signal from the EAPC electrode, suggesting that the EAPC electrode is specific in the detection of catechol and phenol (Fig. 6B).

We examined the feasibility of TYR-based biosensor for detection of phenol in real water samples. The effluent sample was kindly provided from municipal wastewater treatment plant located in Asan city (Republic of Korea). The overall process configuration of wastewater treatment plant was represented in Fig. S4. Briefly, the water sample was taken from the reservoir prior to discharge to stream. The basic effluent quality was summarized in Table S3. As results of electrochemical sensing experiment, the sensitivity of EAPC with CNT addition in real effluent sample was measured to 1100 μA/mMcm^2, which was 93% of the sensitivity in the buffer solution (100 mM PB, pH 6.5). We have successfully demonstrated that EAPC-TYR biosensor with CNTs addition can be employed for the monitoring of phenolic compounds in the actual water-related environment and systems.

We also examined the thermal stability of EAPC electrode on SPE by measuring the sensitivity time-dependently after incubation of the EAPC electrode with additional CNT (90 w/w%) in aqueous solution at 40 °C (Fig. 6C). The EAPC electrode showed an initial drop after two-hour incubation, but maintained its initial sensitivity from 2 h to 12 h incubation at 40 °C. This result suggests that the electrode of EAPC with CNT addition generates reproducible signal once electrode is stabilized with a life-time of at least 10 h.

4. Conclusions

Starting with a simple dispersion of CNTs in aqueous TYR solution, TYR could be immobilized onto intact CNTs via EAPC approach, achieving high enzyme loading and stability. EAPC together with additional CNTs was successfully employed to develop highly sensitive phenol biosensors. Especially, the EAPC electrode on SPE has demonstrated a great potential for on-site detection of environmental pollutants with high sensitivity in both well-organized condition and the real water environments with various interferences. However, the current study examined the performance of TYR-based biosensor in a batch system, representing non-flow system such as tank or reservoir. The future feasibility study of TYR-based biosensor in the flow system, simulating the actual water treatment process, is expected to allow real-time monitoring that can extend its applicability. It is anticipated that the simple dispersion of CNTs in enzyme solution and follow-up fabrication of EAPC on intact CNTs with no acid treatment will create new opportunities not only for mechanistic investigation of CNT dispersion in various biomolecule solution but also for highly sensitive and stable enzyme biosensors to be used for a variety of enzyme-based biosensing applications.

Acknowledgements

This work was supported by the Global Research Laboratory Program (2014K1A1A2043032) and Nano-Material Technology Development Program (2014M3A7B4052193) through the National Research Foundation of Korea (NRF) funded by the Ministry of Science, ICT and Future Planning. This work was also supported by the Korea Institute of Energy Technology Evaluation and Planning (KETEP) and the Ministry of Trade, Industry & Energy (MOTIE) of the Republic of Korea (20182010600430).

Credit author statement

Youngho Wee gave significant efforts to write the review & editing and investigate Figs. 3, 4, 5, 6.

Seunghwan Park gave significant efforts to validate and investigate Figs. 4, 5, 6.

Young Hyeon Kwon gave significant efforts to visualize and write the original draft.

Youngjun Ju gave significant efforts to provide the resource by immobilizing enzyme on CNTs for this manuscript.

Dr. Kyung Min Yeon gave significant efforts to provide the resource the waste water for Fig. 6.

Dr. Jungbae Kim supervised our efforts to conduct the overall experiments of immobilized tyrosinase based biosensors.

Declaration of interests

None.

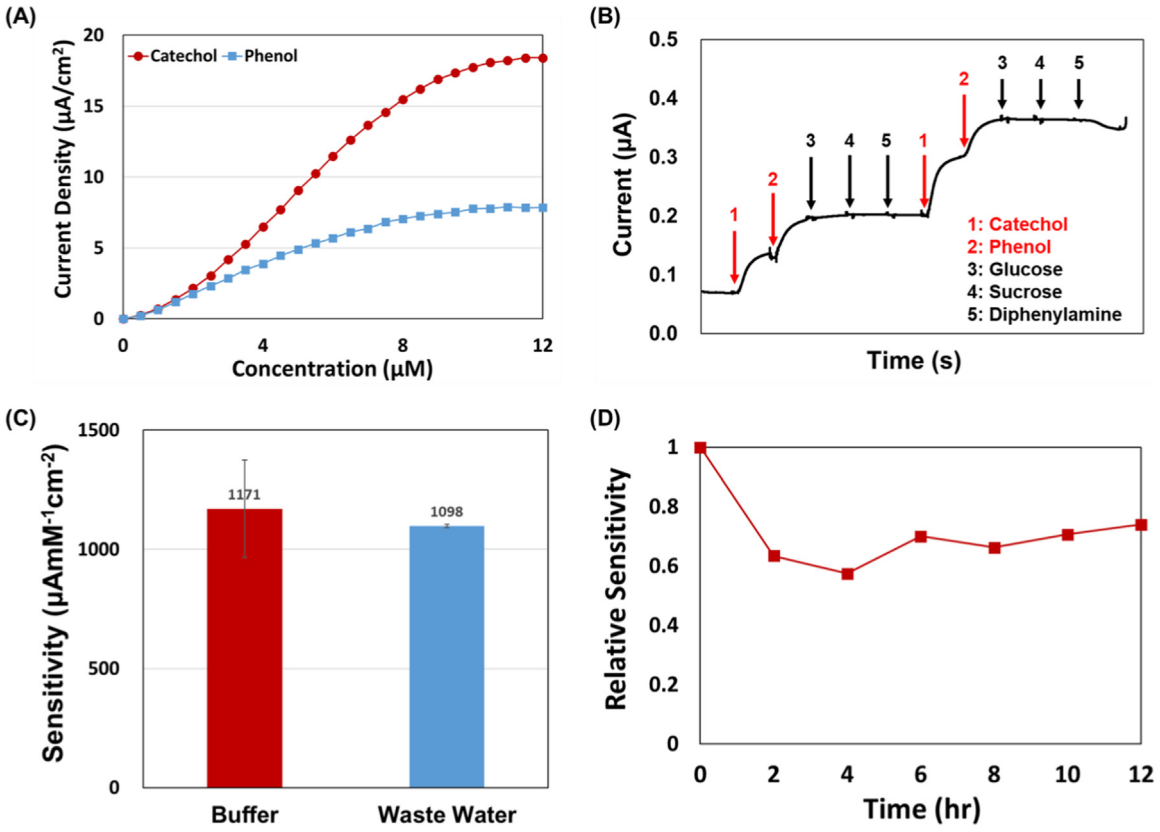

Fig. 6. (A) Calibration curves of current density vs. catechol/phenol concentration, and (B) the specificities of EAPC electrode upon injection of five chemicals (catechol, phenol, glucose, sucrose, and diphenylamine) in a duplicate way. (C) Comparison of sensitivities for phenol in buffer and real waste water, and (D) the sensitivity stability of EAPC electrode with additional CNTs (90 w/w%) on SPE after incubation in an aqueous buffer solution at 40 °C.

Appendix A. Supporting information

Supplementary data associated with this article can be found in the online version at https://doi.org/10.1016/j.bios.2019.03.008.

References

Alarcón, P., Bustos, A., Cañas, B., Andrés, M.D., Polo, L.M., 1987. Chromatographia 24 (1), 613–616.
Angelino, S., Gennaro, M.C., 1997. Anal. Chim. Acta 346 (1), 61–71.
Badihi-Mossberg, M., Buchner, V., Rishpon, J., 2007. Electroanalysis 19 (19-20), 2015–2028.
Baeumner, A.J., 2003. Anal. Bioanal. Chem. 377 (3), 434–445.
Barone, P.W., Baik, S., Heller, D.A., Strano, M.S., 2004. Nat. Mater. 4, 86.
Camargo, J.R., Baccarin, M., Raymundo-Pereira, P.A., Campos, A.M., Oliveira, G.G., Fatibello-Filho, O., Oliveira, O.N., Janegitz, B.C., 2018. Anal. Chim. Acta 1034, 137–143.
Cerrato-Alvarez, M., Bernalte, E., Bernalte-García, M.J., Pinilla-Gil, E., 2019. Talanta 193, 93–99.
Cheaib, D., El Darra, N., Rajha, H., El-Ghazzawi, I., Mouneimne, Y., Jammoul, A., Maroun, R., Louka, N., 2018. Antioxidants 7 (12).
Dai, M., Huang, T., Chao, L., Tan, Y., Chen, C., Meng, W., Xie, Q., 2016. RSC Adv. 6 (21), 17016–17022.
Dalkıran, B., Esra Erden, P., Kılıç, E., 2017. Talanta 167, 286–295.
Datta, S., Christena, L.R., Rajaram, Y.R.S., 2013. 3 Biotech 3 (1), 1–9.
Jacobs, C.B., Peairs, M.J., Venton, B.J., 2010. Anal. Chim. Acta 662 (2), 105–127.
Kim, B.C., Zhao, X., Ahn, H.-K., Kim, J.H., Lee, H.-J., Kim, K.W., Nair, S., Hsiao, E., Jia, H., Oh, M.-K., Sang, B.I., Kim, B.-S., Kim, S.H., Kwon, Y., Ha, S., Gu, M.B., Wang, P., Kim, J., 2011a. Biosens. Bioelectron. 26 (5), 1980–1986.
Kim, B.C., Lee, I., Kwon, S.-J., Wee, Y., Kwon, K.Y., Jeon, C., An, H.J., Jung, H.-T., Ha, S., Dordick, J.S., Kim, J., 2017a. Sci. Rep. 7, 40202.
Kim, H., Lee, I., Kwon, Y., Kim, B.C., Ha, S., Lee, J.-H., Kim, J., 2011b. Biosens. Bioelectron. 26 (9), 3908–3913.
Kim, H., Kim, H.S., Lee, D., Shin, D., Shin, D., Kim, J., Kim, J., 2017b. Anal. Chem. 89 (20), 10655–10660.
Kim, J., Grate, J.W., Wang, P., 2006. Chem. Eng. Sci. 61 (3), 1017–1026.
Kim, J., Grate, J.W., Wang, P., 2008. Trends Biotechnol. 26 (11), 639–646.
Kim, J.H., Jun, S.-A., Kwon, Y., Ha, S., Sang, B.-I., Kim, J., 2015. Bioelectrochemistry 101, 114–119.
Kim, J.H., Hong, S.-G., Wee, Y., Hu, S., Kwon, Y., Ha, S., Kim, J., 2017c. Biosens. Bioelectron. 87, 365–372.
Kim, J.-H., Choi, D.-C., Yeon, K.-M., Kim, S.-R., Lee, C.-H., 2011c. Environ. Sci. Technol. 45 (4), 1601–1607.
Kim, T.H., Lee, I., Yeon, K.-M., Kim, J., 2018. J. Membr. Sci. 554, 357–365.
Kurbanoglu, S., Rivas, L., Ozkan, S.A., Merkoçi, A., 2017. Biosens. Bioelectron. 88, 122–129.
Kwon, K.Y., Yang, S.B., Kong, B.-S., Kim, J., Jung, H.-T., 2010. Carbon 48 (15), 4504–4509.
Lai, J., Yi, Y., Zhu, P., Shen, J., Wu, K., Zhang, L., Liu, J., 2016. J. Electroanal. Chem. 782, 138–153.
Lee, B., Yeon, K.-M., Shim, J., Kim, S.-R., Lee, C.-H., Lee, J., Kim, J., 2014. Biomacromolecules 15 (4), 1153–1159.
Lee, J., Lee, I., Nam, J., Hwang, D.S., Yeon, K.-M., Kim, J., 2017. ACS Appl. Mater. Interfaces 9 (18), 15424–15432.
Martínez, D., Cugat, M.J., Borrull, F., Calull, M., 2000. J. Chromatogr. A 902 (1), 65–89.
Naidja, A., Huang, P.M., Dec, J., Bollag, J.-M., 1999. Effect of Micro. Inter. on Soil and Freshwater Enviro. pp. 181–188.
Portaccio, M., Di Martino, S., Maiuri, P., Durante, D., De Luca, P., Lepore, M., Bencivenga, U., Rossi, S., De Maio, A., Mita, D.G., 2006. J. Mol. Catal. B: Enzym. 41 (3), 97–102.
Sczesny, S., Nau, H., Hamscher, G., 2003. J. Agric. Food Chem. 51 (3), 697–703.
Shahar, H., Tan, L.L., Ta, G.C., Heng, L.Y., 2019. Sens. Actuator B-Chem. 281, 80–89.
Shim, M., Shi Kam, N.W., Chen, R.J., Li, Y., Dai, H., 2002. Nano Lett. 2 (4), 285–288.
Švitel, J., 1998. Environ. Sci. Technol. 32 (6), 828–832.
Tang, L., Zeng, G., Liu, J., Xu, X., Zhang, Y., Shen, G., Li, Y., Liu, C., 2008. Anal. Bioanal. Chem. 391 (2), 679–685.
Tîlmaciu, C.-M., Morris, M.C., 2015. Front. Chem. 3 (59-59).
Tsai, Y.-C., Chiu, C.-C., 2007. Sens. Actuator B-Chem. 125 (1), 10–16.
Vicentini, F.C., Janegitz, B.C., Brett, C.M.A., Fatibello-Filho, O., 2013. Sens. Actuator B-Chem. 188, 1101–1108.
Williamson, K.S., Petty, J.D., Huckins, J.N., Lebo, J.A., Kaiser, E.M., 2002. Chemosphere 49 (7), 703–715.
Willner, I., Yan, Y.M., Willner, B., Tel-Vered, R., 2009. Fuel Cells 9 (1), 7–24.
Wu, L., Deng, D., Jin, J., Lu, X., Chen, J., 2012. Biosens. Bioelectron. 35 (1), 193–199.
Yamazaki, S.-i., Itoh, S., 2003. J. Am. Chem. Soc. 125 (43), 13034–13035.
Zhang, P., Henthorn, D.B., 2009. AIChE J. 56 (6), 1610–1615.
Zhou, Y., Tang, L., Zeng, G., Chen, J., Cai, Y., Zhang, Y., Yang, G., Liu, Y., Zhang, C., Tang, W., 2014. Biosens. Bioelectron. 61, 519–525.